Applied Catalysis A: General 346 (2008) 140–148

Contents lists available at ScienceDirect

Applied Catalysis A: General

journal homepage: www.elsevier.com/locate/apcata

Comparison of catalytic decomposition of hydrogen peroxide and catalytic degradation of phenol by immobilized iron oxides

Chun-Ping Huang [a], Yao-Hui Huang [a,b,*]

[a] Department of Chemical Engineering, National Cheng Kung University, 1 Ta-Hsueh Road, Tainan City 701, Taiwan
[b] Sustainable Environment Research Center, National Cheng Kung University, Tainan City 701, Taiwan

ARTICLE INFO

Article history:
Received 9 November 2007
Received in revised form 5 May 2008
Accepted 14 May 2008
Available online 20 May 2008

Keywords:
Catalyst
Phenol
Iron oxides
Fenton
Fluidized bed reactor

ABSTRACT

Immobilized iron oxides on silica matrixes in fluidized bed reactors, including SiG1, SiG2, C1, and the commercial catalyst FeOOH, were used in the catalytic decomposition of H_2O_2 and the catalytic degradation of phenol. They were characterized using XRD, SEM, N_2-sorption, and elucidation of the kinetics of dissolved iron by oxalic acid in dark surroundings. XRD patterns reveal that SiG1, SiG2, and C1 exhibit amorphous structures, and FeOOH exhibits the poor crystallinity of goethite. The SEM images reveal that the surfaces of all the iron oxides are smooth and that the iron oxides are aggregated by the iron oxide floc. The N_2-sorption isotherm indicates that SiG1 and SiG2 are non-porous materials, and that C1 and FeOOH are typical type II and typical type IV materials, respectively. A kinetic model for iron dissolved by oxalic acid is established. The order of apparent first-order dissolution rate constants (k_c) is SiG1 > SiG2 > FeOOH ~ C1. The immobilized iron oxides, SiG1 and SiG2, are weakly bonded to the support (silica sand) in the presence of oxalic acid. The decomposition of H_2O_2 follows pseudo-first-order kinetics. The number of active sites for the decomposition of H_2O_2 is similar among all iron oxides at a particular k_{app} (1.8×10^{-3} min^{-1}). There are no interactions between phenol and iron oxides in the absence of hydrogen peroxide at pH 4. SiG1 and SiG2 exhibit much higher catalytic activities in phenol degradation than either C1 or FeOOH. The reactivity of iron oxides in catalyzing the phenol degradation by H_2O_2 relates to the tendency of iron to be dissolved by oxalic acid. The intermediates of phenol degradation, such as catechol and oxalic acid, promote the dissolution of iron from SiG1 and SiG2 by reductive and non-reductive pathways and lower the pH values. The catalyses of SiG1 and SiG2 involve heterogeneous and homogeneous reactions.

1. Introduction

Hydrogen peroxide is green, efficient, easy to use, and suitable for use in the remediation of contamination. However, hydrogen peroxide alone is not an excellent oxidant of most organic substances so the activation of hydrogen peroxide is an issue. Transition metal ions, such as iron ions, are widely employed to catalyze hydrogen peroxide, generating the very reactive hydroxyl free radical [1]. The mixture of ferrous salts and hydrogen peroxide is known as Fenton's reagent:

$$Fe(III) + H_2O_2 \rightarrow Fe(III) + {}^{\bullet}OH + OH^- \quad (1)$$

Application of Fenton's reagent in the destruction of organic compounds is limited by the slurry system because it produces a significant amount of ferric hydroxide sludge, which requires further separation and disposal. Iron oxides have been recently applied for the degradation or mineralization of organic contaminants with hydrogen peroxide [2–5]. The major advantages of iron oxides are that they are economical and easy to activate; as heterogeneous catalysts, they can also be easily separated from treated wastewater. Various types of iron oxides exhibit various chemical activities. Additionally, hydrogen peroxide, which is activated by iron oxide, is usually related to the Fenton-like system:

$$Fe(III) + H_2O_2 \rightarrow Fe(HO_2)^{2+} + H^+ \quad (2)$$

$$Fe(HO_2)^{2+} \rightarrow Fe(II) + HO_2^{\bullet} \quad (3)$$

The Fe(II) can be slowly generated by reactions (2) and (3). However, the consumption rate of H_2O_2 does not equal the

* Corresponding author at: Department of Chemical Engineering, National Cheng Kung University, 1 Ta-Hsueh Road, Tainan City, Taiwan.
Tel.: +886 6 2757575x62636; fax: +886 6 2344496.
E-mail address: yhhuang@mail.ncku.edu.tw (Y.-H. Huang).

0926-860X/$ – see front matter © 2008 Elsevier B.V. All rights reserved.
doi:10.1016/j.apcata.2008.05.017

generation rate of hydroxyl radicals because hydrogen peroxide can be decomposed to water and oxygen via non-radical-producing pathways by iron oxides [6]. Therefore, some effective iron oxides that can transform hydrogen peroxide to generate the hydroxyl radical must be found. Cunningham et al. noted that amorphous iron oxides appear to be much more reactive than crystalline oxides in the presence of light [7]. Goethite (α-FeOOH) has recently been found to catalyze the effective oxidation of organic compounds by hydrogen peroxide [8]. Valentine compared three iron oxides as catalysts of the oxidation of quinoline by hydrogen peroxide; goethite was the most effective [4]. Heterogeneous catalysts based on magnetic mixed iron oxides have been used to decolorize several synthetic dyes [9]. Iron species are incorporated over different silica supports for the heterogeneous photo-Fenton oxidation of phenol [10]. A series of iron oxide nano-particles immobilized on a resin has been reported to have high hydroxylation activity due to the formation of nano-sized β-FeOOH particles inside resins [11]. A highly ordered iron-containing mesoporous material, Fe-MCM-41, has been prepared to oxidize phenol using H_2O_2 [12]. Crowther and Larachi supported iron(III) species on silica-based mesoporous molecular sieves, and used them as catalysts of the degradation of phenol [13]. Melero et al. supported a nanocomposite solid catalyst that included mixtures of crystalline iron oxides over a silica SBA-15 matrix. It was used as an effective catalyst of the degradation of phenolic solution [14,15]. The authors also pointed out that the development of highly stable active materials that are effective over a wide pH range is a challenge in the oxidation of organic compounds in the presence of hydrogen peroxide. However, immobilized iron oxide nano-particles are expensive and difficult to scale-up for the treatment of wastewater. The fluidized bed reactor Fenton (FBR Fenton) process has been established in Taiwan to minimize the production of iron sludge. Iron oxides derived from the FBR Fenton process are cheaper, recyclable, plentiful and more active. The immobilized iron oxides derived from the FBR Fenton process exhibit high activity in catalyzing oxidation of organic compounds by hydrogen peroxide under ambient conditions. A novel supported γ-FeOOH catalyst was developed, and the researchers demonstrated that it can effectively catalyze the oxidation of benzoic acid by H_2O_2 in a fluidized bed reactor [16]. In our previous work, the iron oxide material, which is a by-product of the FBR-Fenton reaction that was used in the treatment of the bioeffluent of tannery wastewater from a dyeing/finishing plant in Taiwan, efficiently degraded reactive black 5 [17,18].

This work compares the oxidations of the model pollutant, phenol, by hydrogen peroxide in the presence of four iron oxides. Phenol is present in the wastewater that is discharged in the resin manufacturing, petrochemical, oil-refining, paper-making, coking, and iron-smelting industries. Reducing the amount of phenol in phenolic wastewater to harmless levels is an arduous task that involves many biological and chemical processes because of phenol's high solubility and stability in water [19]. Three of the immobilized iron oxides on silica matrixes utilized in this study, SiG1, SiG2, and C1, were prepared in fluidized bed reactors. The other iron oxide is the commercial catalyst FeOOH, obtained from the Aldrich Chemical Company. Notably, SiG2 has been successfully adopted in Taiwan to purify ground water that has been polluted by phenol. The characteristics of these iron oxides were investigated using SEM, XRD, and BET. The kinetics of the dissolution of iron by oxalic acid, which reflect the crystallinity and the bond strength between the iron oxide and the support, have been established. The kinetics of H_2O_2 decomposition is studied first to compare the reactivity of these iron oxides. The comparison of iron oxides with their reactivity in terms of the efficiency of phenol degradation is based on a fixed consumption rate of H_2O_2. Such intermediates as catechol and 1,4-hydroquinone from the oxidation of phenol are regarded as reductants of aqueous Fe^{3+} [20–22]. These intermediates accelerate the decomposition of H_2O_2 and the degradation of phenol, so reductive dissolution of iron oxides in the presence of aqueous catechol solution need to be studied. The variation of pH and the extent of dissolution of iron oxide are determined.

2. Method

2.1. Synthesis of iron oxides and materials

A novel catalyst, iron oxide on a silica sand support, was developed in the following manner [23]. The ferrous ions in ground water were oxidized by aerated air, and the iron oxide was simultaneously immobilized on non-porous silica sand at neutral pH in a fluidized bed reactor. The iron oxide was withdrawn from the fluidized bed reactor after 1 month (SiG1) and 1 year (SiG2). The synthetic ferrous ions in water solution were oxidized by hydrogen peroxide, and the iron oxide was then immobilized on silica-based ceramic particles at acidic pH in a fluidized bed reactor. The iron oxide was withdrawn from the fluidized bed reactor after 4 months. The commercial iron oxide catalyst FeOOH (30–50 mesh) was purchased from the Aldrich Chemical Company. Table 1 lists the physical properties of these iron oxides. Phenol (90%, Riedel-de Haën), Catechol (99+%, Acros) and H_2O_2 (30%, Riedel-de Haën) were analytical reagent grade and were used without further purification.

2.2. Characterization of iron oxides

The crystallinity of the iron oxides was measured using X-ray diffraction with Cu Kα radiation (Rigaku RX III). The morphology of the iron oxides was examined using SEM (JEOL JSM-6700F). The specific surface area was determined using the BET method.

2.3. Kinetics of dissolution of iron by oxalic acid and H_2O_2 decomposition

SiG1 (1.00 g), SiG2 (1.00 g), C1 (0.50 g), and FeOOH (0.20 g) were added into 1-L beakers that contained 1 mM oxalic acid at pH 3.0 with an agitation speed of 150 rpm in dark surroundings. The samples were withdrawn after a period and filtered using a 0.2-μm membrane filter (cellulose acetate, Advantec). The dissolved iron was analyzed using an atomic analyzer (GBC).

Ten, 20, 30 and 50 g of SiG1 were added to 1-L beakers that contained 10 mM $NaClO_4$ (ionic strength) in 1-L solutions; H_2O_2 (550 mg/L) was then added to initiate the reaction at pH 4 (adjusted by $HClO_4$) at 30 °C with an agitation speed of 150 rpm. Immediately after filtration, the H_2O_2 concentration in the filtrate was measured using the titanium sulfate method [24]. SiG2 (10, 20,

Table 1
Physical properties of iron oxides

	SiG1	SiG2	C1	FeOOH
Parameter				
Support	Silica	Silica	Ceramic	None
Total iron content of catalyst (g/kg)	17.09	56.93	308.4	628.5
Bulk density (g/cm^3)[a]	1.52	1.58	1.45	1.48
Absolute (true) density (g/cm^3)[b]	2.42	2.63	2.89	3.48
Specific surface area (m^2/g)	1.29	5.35	117.7	102.1
Mean particle diameter (mm)	0.99	0.89	0.67	0.46
Total pore volume (ml/g)	0.0062	0.0051	0.1080	0.2051

[a] Mass of solid divided by volume of solid and void.
[b] Mass of solid divided by volume of solid.

30 and 50 g), C1 (1, 2, 3, 5 and 10 g), and FeOOH (0.5, 1, 1.5 and 2 g) were also adopted in the decomposition of H_2O_2 (550 mg/L) under the same conditions with the same steps as SiG1.

2.4. Degradation of phenol and reductive dissolution of iron in presence of catechol

Various iron oxides were added into 1-L beakers that contained 10 mM $NaClO_4$ (ionic strength) and phenol (100 mg/L, 1.06 mM) in 1-L solution; H_2O_2 (550 mg/L, 16.18 mM) was then added to initiate the reaction at initial pH 4 (adjusted by $HClO_4$) and 30 °C with an agitation speed of 150 rpm. The samples were withdrawn after a period and filtered using a 0.2-μm membrane filter. The phenol concentration was measured using HPLC with a TSK-GEL ODS-100S column (4.6 mm × 250 mm) and a UV detector at 225 nm. The mobile phase was methanol/water = 4/6.

SiG1 (20 g), SiG2 (20 g), C1 (2 g) and FeOOH (0.5 g) were immersed in 1-L aqueous catechol (50 mg/L) solutions that contained 10 mM $NaClO_4$ (ionic strength) at pH 4 (adjusted by $HClO_4$) at 30 °C with an agitation speed of 150 rpm. The samples were withdrawn after a period of time and filtered using a 0.2-μm membrane filter. The concentration of ferrous ions was measured using the 1,10-phenathroline method [25].

3. Results and discussion

3.1. Catalyst properties

Fig. 1 shows the XRD patterns of four iron oxides, standard goethite, and the SiO_2 support of SiG1 and SiG2. The synthetic iron oxides, SiG1 and SiG2 and C1, exhibited an amorphous structure because of the moderate temperature preparation ambient (room temperature), whereas the commercial iron oxide FeOOH was associated with the poor crystallinity of goethite. Fig. 2 displays the morphologies of the iron oxides. The surfaces of all the iron oxides are smooth; the oxides are aggregated by the iron oxide floc. The enlarged micrographs reveal that the catalysts have similar morphologies because these iron oxides exhibit poor crystallinity. Unlike crystalline iron oxides, the amorphous iron oxides are difficult to distinguish using XRD and SEM. Furthermore, the stability of iron oxide can be examined by oxalic acid and will be discussed in the following section. Table 1 presents the physical properties of these iron oxides—mean particle diameter, density, specific area of BET and total pore volume. These iron oxides all have mean particle diameters and densities, so the mixing conditions of solids in each reactor should be similar. The specific areas of SiG1 and SiG2 are quite low, indicating that the internal diffusion of solutes is negligible. The surface area is believed to be proportional to the number of active sites of the solids for reaction, adsorption and desorption processes. Fig. 3 plots the N_2-adsorption isotherm, corresponding to typical type II for C1 and typical type IV for FeOOH. The adsorbed volumes for SiG1 and SiG2 are quite low because of non-porosity.

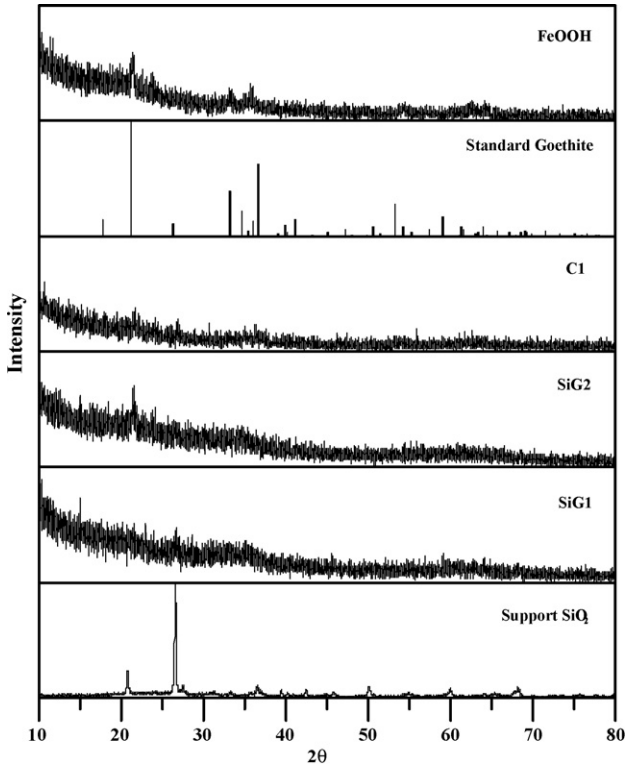

Fig. 1. XRD patterns of SiG1, SiG2, C1 and FeOOH.

3.2. Kinetics of dissolution of iron by oxalic acid

The dissolution rates of highly crystalline iron oxides are typically lower than those of poorly crystalline iron oxides in the presence of oxalate [26]. The reactivity of iron oxides, as reflected by their tendency to dissolve, is very important to both the redox cycling of iron and the bioavailability of iron to phytoplankton in natural waters [27]. Whether the tendency for iron oxide to dissolve relates to the reactivity of phenol degradation is thus of interest. However, most works have involved the preparation of highly ordered or crystalline iron oxides for the use of catalysts to prevent iron leaching. A major challenge is that iron leaching is caused by lower pH, complex dissolution or reductive dissolution during the oxidation of organic compounds. Oxalic acid is always generated and forms a complex with iron during the degradation of organic compounds. The non-reductive dissolution of iron oxides occurs in aqueous oxalic acid solution and dark surroundings [28]. In this work, iron oxides were non-reductively dissolved in aqueous oxalic acid (1.0 mM) at pH 3.0 in dark surroundings. The dissolved iron is defined as the iron species in the filtrate after the material has passed through a 0.2-μm membrane filter. The non-reductive dissolution pathway of iron oxide is simple desorption [28]. The immobilized iron ($[Fe]^{III}_{solid}$) is dissolved by oxalic acid, and ferric complex ions ($[Fe]^{III}_{solution}$) are produced in the oxalic acid solution:

$$Fe^{III}_{solid} \xrightarrow{\text{oxalic acid}\ (k_c)} Fe^{III}_{solution} \quad (4)$$

The rate of dissolution iron oxide is proportional to the concentration gradient of iron between solid and solution (driving force), so the kinetic model of the dissolution of iron by oxalic acid can be expressed as

$$\frac{d[Fe]_{solid}}{dt} = -k_c[Fe]_{solid} \quad (5)$$

$$[Fe]_{solid} = [Fe]_{solid,0} - [Fe]_{solution} \quad (6)$$

No iron is dissolved in the solution at time zero (i.e. $[Fe]_{solution,0} = 0$). Therefore:

$$-\ln\left(1 - \frac{[Fe]_{solution}}{[Fe]_{solid,0}}\right) = k_c t \quad (7)$$

where k_c is the apparent first-order dissolution rate constant of iron oxide; t is time, and subscript "0" refers to time zero. $[Fe]_{solid}$ and $[Fe]_{solution}$ are the concentrations of iron in solid and solution,

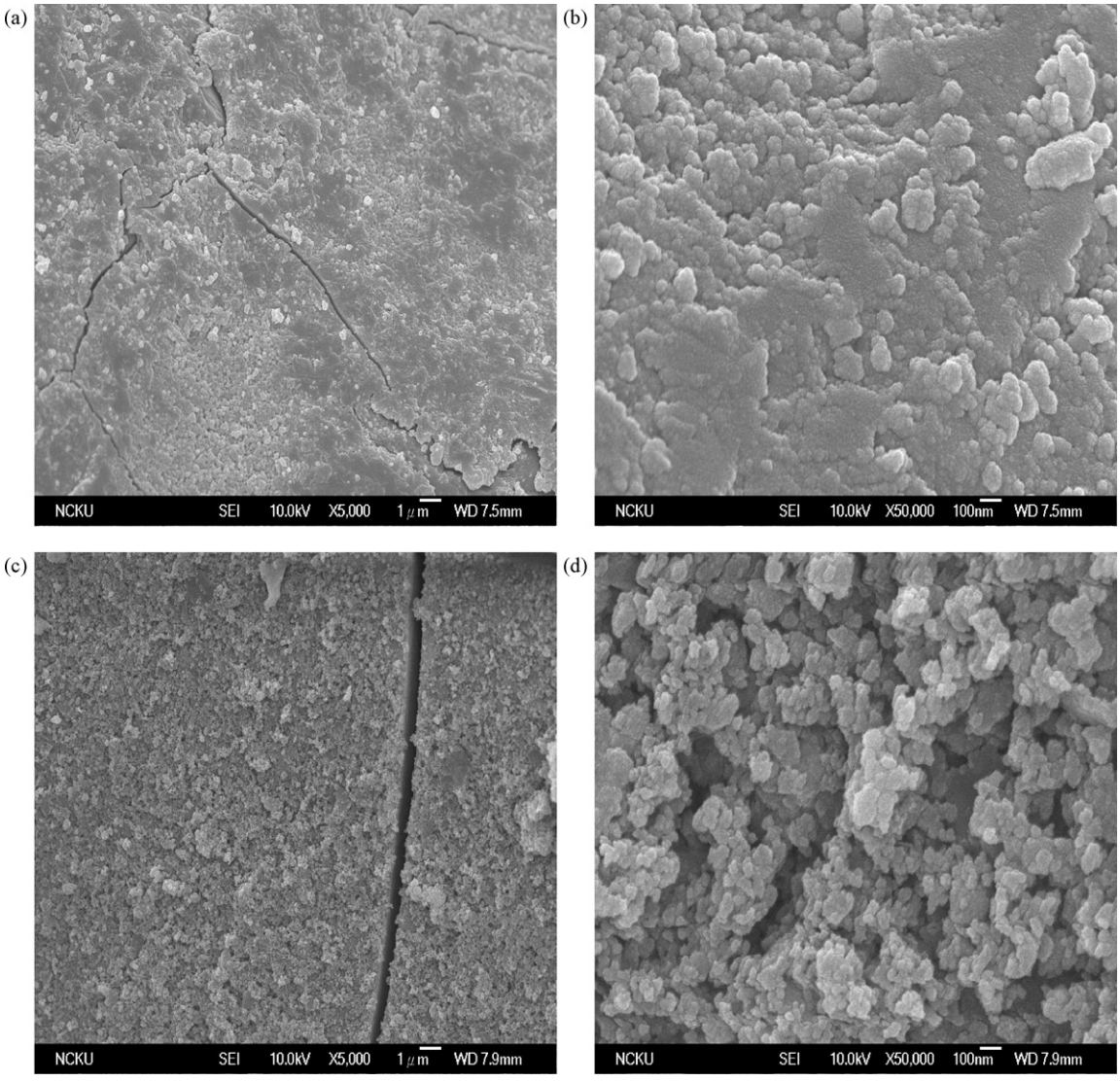

Fig. 2. SEM images of iron oxides (a) SiG1 5000×, (b) SiG1 50,000×, (c) SiG2 5000×, (d) SiG2 50,000×, (e) C1 5000×, (f) C1 50,000×, (g) FeOOH 5000×, and (h) FeOOH 50,000×.

respectively. SiG1 and SiG2 were withdrawn from the same fluidized bed reactor with different times; hence, the kinds of iron species should be similar. The same weight of samples (1 g) is selected to compare the solubility values of SiG1 and SiG2 at different amounts of immobilized iron species (driving force) in the presence of oxalic acid. C1 (0.5 g) and FeOOH (0.2 g) contain approximate amounts of iron species so the solubility values depend on their nature (k_c).

The lines in Fig. 4 were fitted to the data by linear regression, yielding correlation coefficients >0.980 and the kinetics parameters that are presented in Table 2. About 40% (6.8 mg L^{-1}), 18% (10.3 mg L^{-1}), 4.0% (6.3 mg L^{-1}) and 3.7% (4.2 mg L^{-1}) of the immobilized iron in SiG1, SiG2, C1 and FeOOH, respectively, dissolved in 300 min. The apparent first-order dissolution rate constant of iron oxide (k_c) yields the solubility of iron oxide in 1.0 mM aqueous oxalic acid solution and the bonding strength between the iron oxide and the support. The immobilized iron oxides, SiG1 and SiG2, dissolve more easily in the presence of oxalic acid because the bonding between iron oxide and the support (silica sand) is weak, and the bonding strength of SiG2 is stronger than that of SiG1. Since C1 contains much more iron oxide than either SiG1 or SiG2, its properties closely resemble those of FeOOH (without support). The apparent first-order dissolution rate constant (k_c) reveals an important property of iron oxide that is dissolved by oxalic acid. In this work, k_c values follow the order SiG1 > SiG2 > FeOOH ~ C1. When the degradation of organic compounds proceeds, carboxylic acids, including oxalic acid, are the major intermediates. Therefore, the dissolution of iron oxide is expected in this stage.

3.3. Kinetics of H_2O_2 decomposition

The rate limiting reaction is believed to be the initial reaction between hydrogen peroxide and the iron oxides [3,4,29]. Additionally, the results reveal that the decomposition of H_2O_2 follows pseudo-first order kinetics:

$$-\frac{d[H_2O_2]}{dt} = k_{app}[H_2O_2] \quad (8)$$

and thus:

$$\ln\frac{[H_2O_2]}{[H_2O_2]_0} = -k_{app}t \quad (9)$$

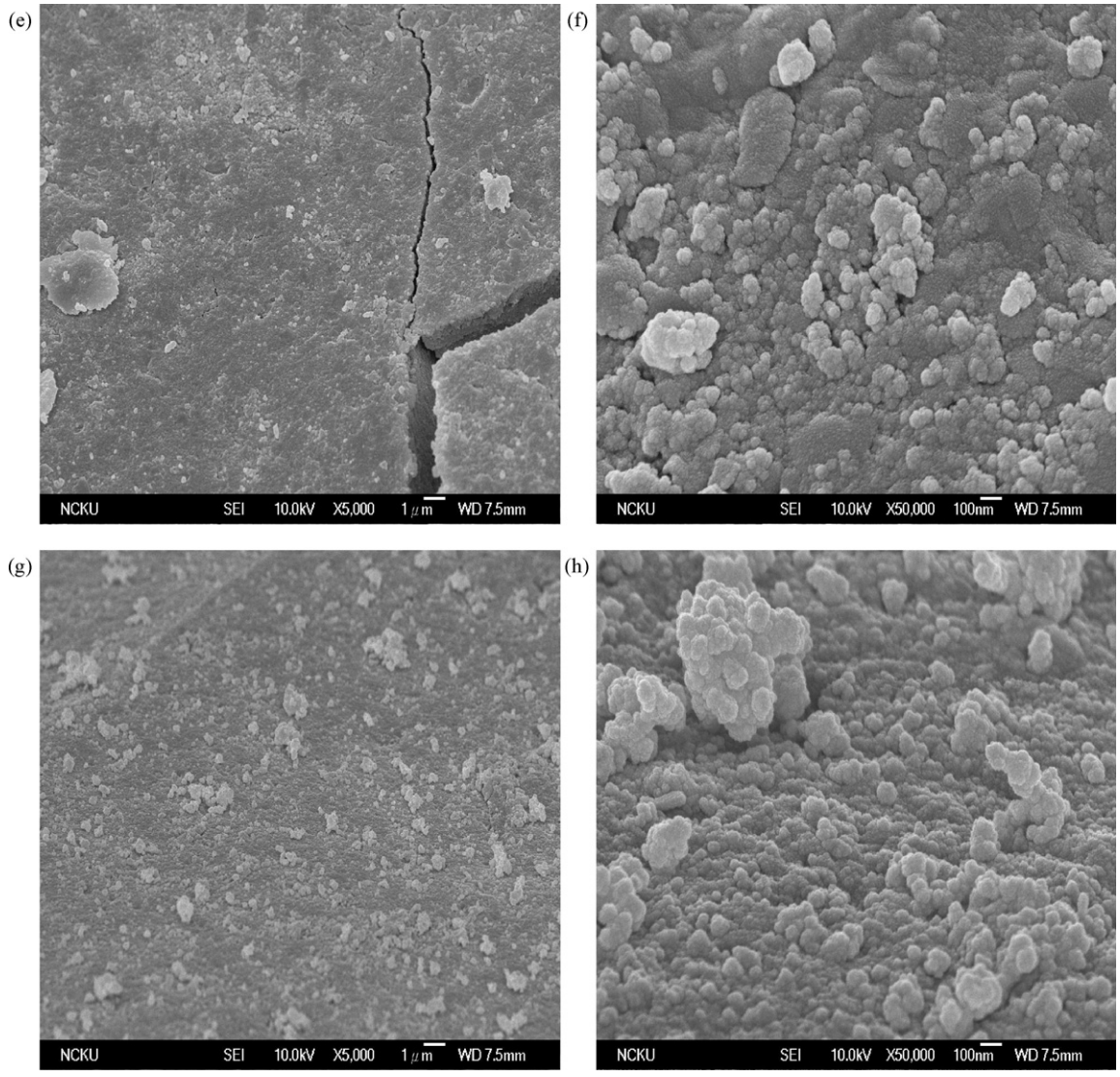

Fig. 2. (*Continued*).

where k_{app} is the apparent first-order rate constant, and $[H_2O_2]$ and $[H_2O_2]_0$ are the concentrations of H_2O_2 in the solution at any time t and time zero, respectively. The lines in Fig. 5a were fitted to the data by linear regression, yielding correlation coefficients >0.980. The apparent first-order rate constants are proportional to the amount of iron oxides (Fig. 5b). Actually, no dissolved iron was measured for all the iron oxides at pH 4.0 and the pH value did not change during the decomposition of H_2O_2. The consumption rate of H_2O_2 depends on the surface area and on the type of iron oxide. Additionally, the generation rate of $^{\bullet}OH$ is proportional to the rate of consumption of H_2O_2 and to the surface area of the iron oxide [6]. However, the consumption rate of H_2O_2 does not equal the generation rate of $^{\bullet}OH$ because H_2O_2 can be decomposed to water and oxygen by iron oxides via a non-radical-producing pathway. When the apparent first-order rate constant is fixed at 1.8×10^{-3} min^{-1}, the applied amounts of iron oxides are 0.5, 2.0, 20 and 20 g for FeOOH, C1, SiG1, and SiG2, respectively. The number of active sites for the decomposition of H_2O_2 is similar to that of those for iron oxides at the same k_{app} (1.8×10^{-3} min^{-1}). Furthermore, the aforementioned amounts of iron oxides were used for the oxidative degradation of phenol in the following experiments. In this section, k_{app} describes a property of iron oxide for the surface reaction with hydrogen peroxide, but it does not refer to whether active radicals are generated by each of these iron oxides. The reactivities of these iron oxides are compared to determine, which can initiate hydrogen peroxide via a radical pathway.

3.4. Phenol degradation and H_2O_2 depletion

The adsorption of phenol and the presence of dissolved iron in the presence of iron oxides were examined. Neither the adsorption of phenol nor any dissolved iron was observed in 5 h (data not shown). On the other hand, there are no interaction between phenol and iron oxides in the absence of hydrogen peroxide. Fig. 6 shows that SiG1 and SiG2 effectively catalyze the degradation of phenol by hydrogen peroxide (about 99% conversion at 180 min), while C1 and FeOOH are ineffective. An obvious lag phase occurred during the degradation of phenol in the initial reaction. Lu found that the initial rate of degradation of 2-chlorophenol was slow in the presence of goethite [8]. Gallard and De Laat also observed a lag phase in the degradation of atrazine in homogeneous Fe(III)/H_2O_2 solution. The phenomenon was explained by the fact that the production of Fe(II) and $^{\bullet}OH$ (Eqs. (1)–(3)) is very slow [30]. The lag

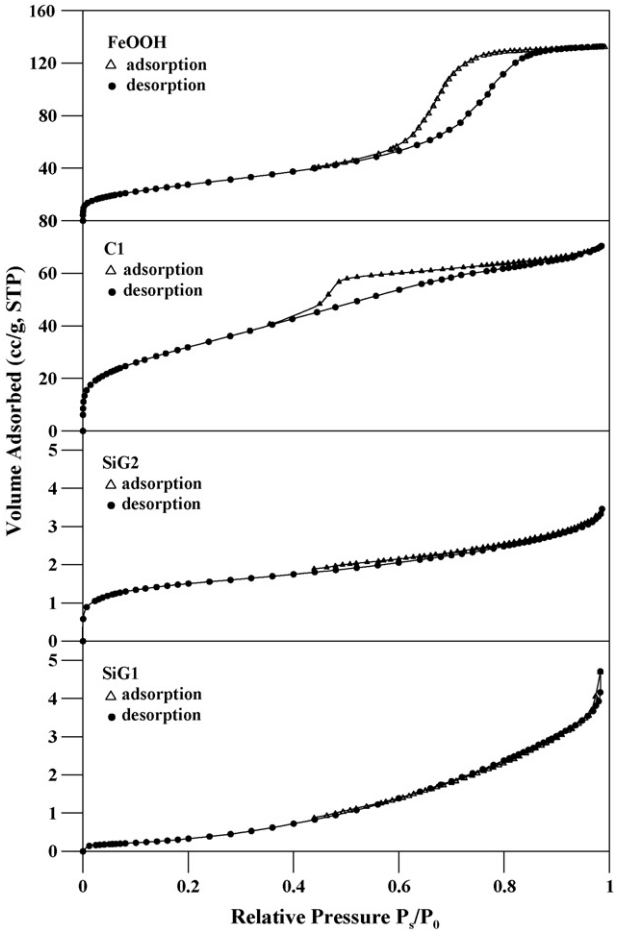

Fig. 3. N_2-sorption isotherms of SiG1, SiG2, C1 and FeOOH.

phase of phenol degradation actually represents a slow rate-limiting reduction of Fe(III) by H_2O_2 (Eqs. (2) and (3)) to Fe(II), which sustains the Fenton reaction (Eq. (1)) [20]. In a heterogeneous system, the induction period of a reaction may involve the diffusion of solutes (H_2O_2 and phenol) and the dissolution of iron

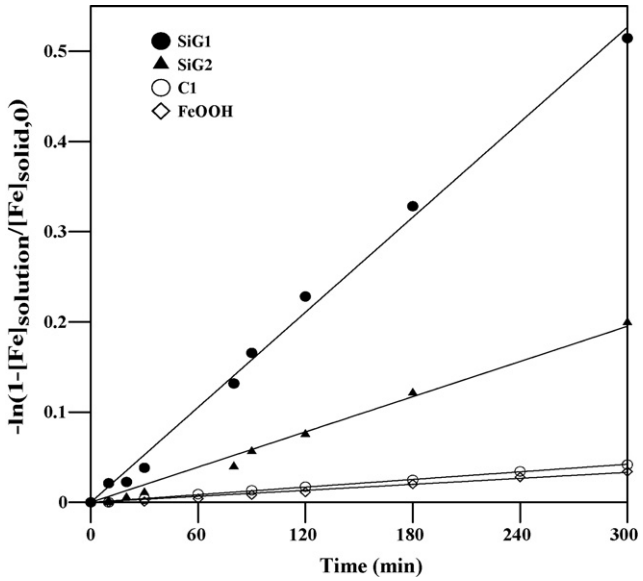

Fig. 4. Kinetics of dissolution of iron by oxalic acid (oxalic acid = 1.0 mM, 30 °C, pH = 3.0, 150 rpm, dark surroundings).

Table 2
Kinetics rate constants and parameters of iron oxides dissolved by oxalic acid

	SiG1 (1 g)	SiG2 (1 g)	C1 (0.5 g)	FeOOH (0.2 g)
Parameter				
$[Fe]_{solid,0}$ (mg/L)[a]	17.09	56.93	154.2	125.7
$[Fe]_{solution,300}$ (mg/L)[b]	10.3	6.8	6.3	4.2
k_c ($\times 10^4 min^{-1}$)	17.56	6.65	1.41	1.11

Oxalic acid = 1.0 mM, 30 °C, pH = 3.0, 150 rpm, dark surroundings.
[a] Concentration of iron in solid at time zero.
[b] Concentration of iron in solution at 300 min.

oxide [12]. Following this induction period, first-order decay was observed in phenol degradation, indicating that the active radicals were produced in steady state and degraded phenol. SiG1 and SiG2 are efficient enough to decompose hydrogen peroxide via a radical pathway for the degradation of phenol, while most of the hydrogen peroxide is decomposed to oxygen and water by C1 and FeOOH. The larger the amounts of C1 and FeOOH that were used, the more H_2O_2 were consumed, but materials were still inefficient for the degradation of phenol. Fig. 7 shows that the decomposition rates of H_2O_2 during the degradation of phenol for SiG1 and SiG2 exceed those of the system without phenol. The decomposition of H_2O_2 still follows pseudo-first-order kinetics, but the apparent rate

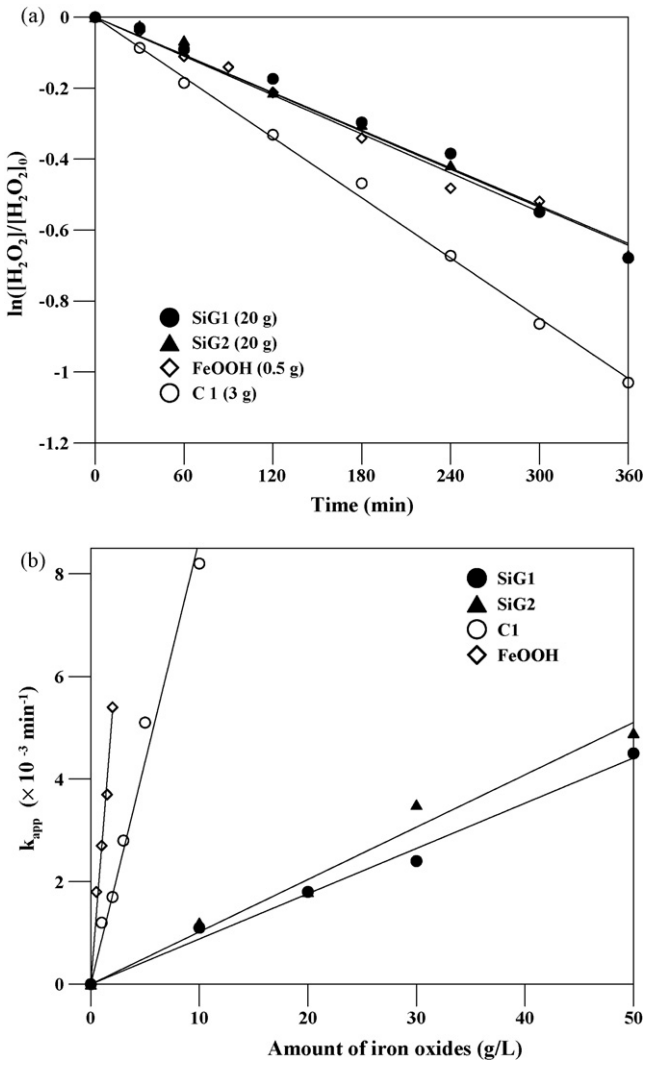

Fig. 5. (a) Decomposition kinetics of H_2O_2 with different iron oxides; (b) various k_{app} values with different amounts of iron oxides (pH = 4.0, 30 °C, $NaClO_4$ = 10 mM, H_2O_2 = 550 mg/L, 150 rpm).

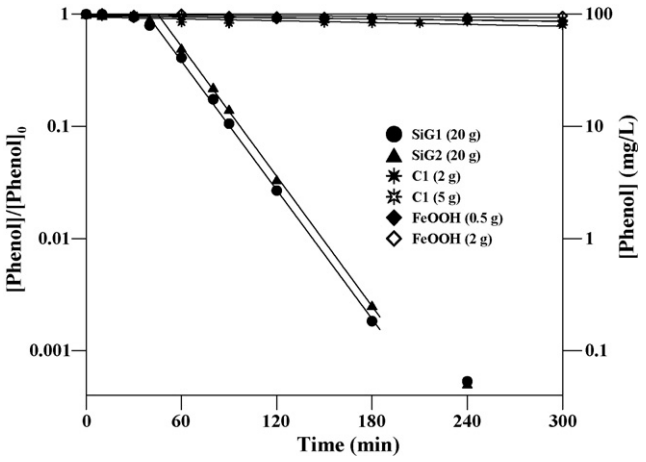

Fig. 6. Phenol degradation by iron oxide catalytic H_2O_2 (pH_i = 4.0, 30 °C, $NaClO_4$ = 10 mM, H_2O_2 = 550 mg/L, phenol = 100 mg/L, 150 rpm).

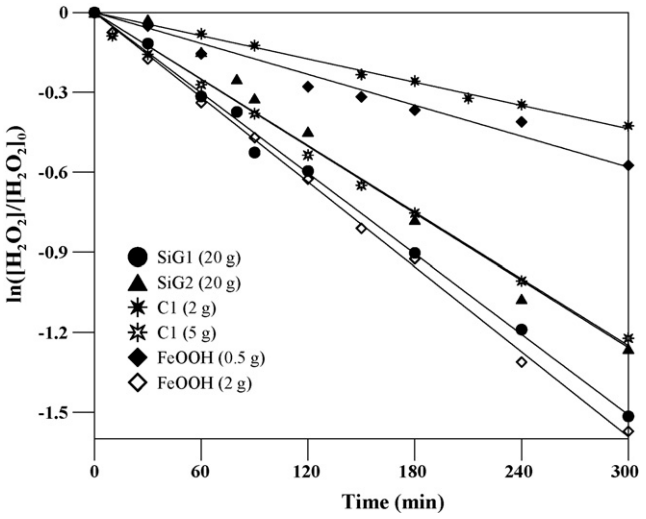

Fig. 7. Decomposition of H_2O_2 during phenol degradation (pH_i = 4.0, 30 °C, $NaClO_4$ = 10 mM, H_2O_2 = 550 mg/L, phenol = 100 mg/L, 150 rpm).

Table 3
k_{app} for different amounts of iron oxides in phenol degradation (H_2O_2 = 550 mg/L, phenol = 100 mg/L, pH_i = 4.0, 30 °C, $NaClO_4$ = 10 mM, 150 rpm)

	k_{app} ($\times 10^3 min^{-1}$)
SiG2 (20 g)	5.0
SiG2 (20 g)	4.5
C1 (2 g)/(5 g)	1.4/4.2
FeOOH (0.5 g)/(2 g)	1.9/5.3

constants are 5×10^{-3} and 4.5×10^{-3} min^{-1} for SiG1 and SiG2, respectively (Table 3). Therefore, the rate of decomposition of H_2O_2 increased during the degradation of phenol. The major products of phenol oxidation are catechol and 1,4-hydroquinone [31]. These species play an important role in reducing Fe(III) to Fe(II) [12,20–22,31–33]. As more Fe(II) is produced, the depletion of H_2O_2 in this stage is faster because the decomposition rate of H_2O_2 by Fe(II) markedly exceeded that by Fe(III). However, the degradation of phenol and the decomposition of H_2O_2 are accelerated by catechol and 1,4-hydroquinone. However, the solubility of Fe(II) is much higher than that of Fe(III) in solution, so iron is expected to dissolve. Additionally, heterogeneous and homogeneous processes during the degradation of phenol proceed simultaneously in SiG1 and SiG2 systems. The following section discusses the reductive and the non-reductive dissolution of iron by catechol and oxalic acid.

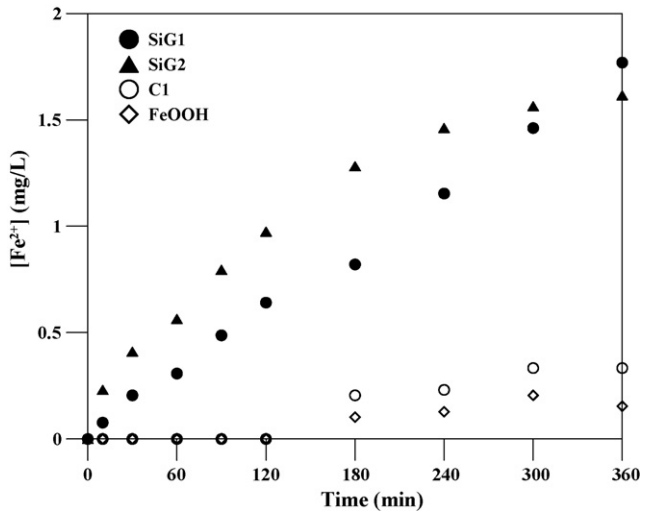

Fig. 8. Reductive dissolution of iron oxides in the presence of catchol (pH = 4.0, 30 °C, $NaClO_4$ = 10 mM, catechol = 50 mg/L, 150 rpm).

3.5. Dissolved iron and pH variation

The hydrogen ions dissociate from the intermediates of the oxidative degradation of phenol, such as aliphatic acids and

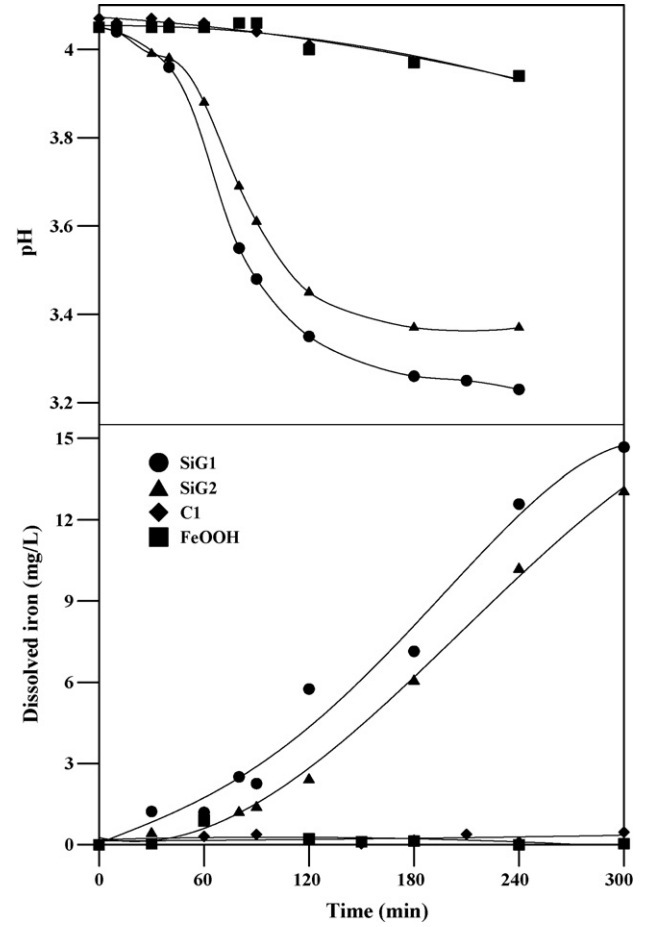

Fig. 9. pH variation and iron dissolution during phenol degradation (pH_i = 4.0, 30 °C, $NaClO_4$ = 10 mM, H_2O_2 = 550 mg/L, phenol = 100 mg/L, 150 rpm).

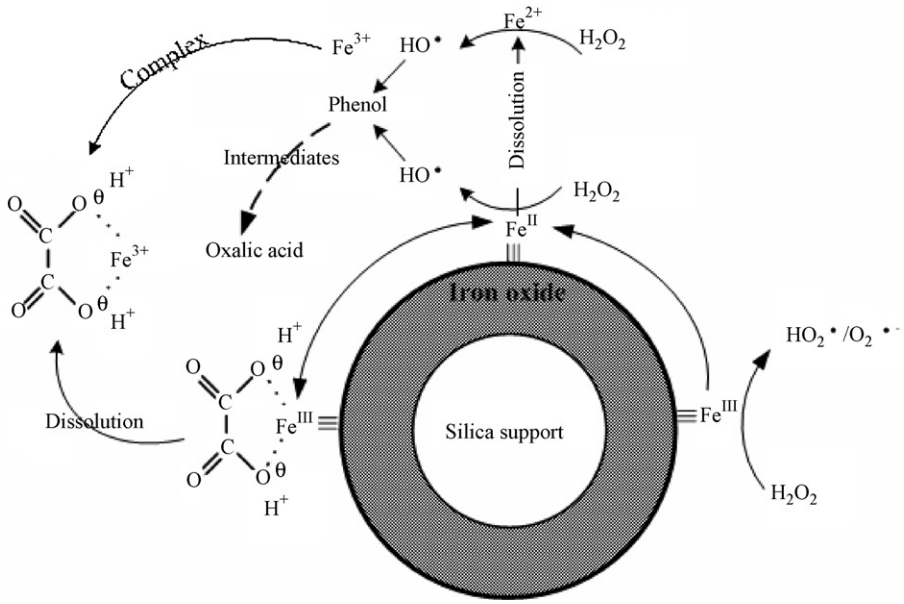

Scheme 1. The probably heterogeneous and homogeneous reactions for SiG1 and SiG2 in the presence of hydrogen peroxide and phenol.

carboxylic acids, decreasing the pH and increasing the solubility of iron [8,34]. The iron oxides are dissolved by organic acids via a non-reductive dissolution pathway, by a mechanism that is similar to that of the dissolution of iron by oxalic acid mentioned in a preceding section [28]. Some of the intermediates that are derived from phenol degradation, such as catechol and 1,4-hydroquinone, reduce Fe(III) to Fe(II) and result in the reductive dissolution of iron. When ferric ions are mixed with aqueous catechol solution, ferrous ions are produced immediately (data not shown) because ferric ions react with catechol rapidly (pH < 3), a fact which is consistent with the literature [20]. In the light of the Fe^{3+}/catechol test, the reductive dissolution of iron oxides in the presence of catechol can be studied. SiG1 (20 g), SiG2 (20 g), C1 (2 g) and FeOOH (0.5 g) were immersed in aqueous catechol (50 mg/L) solutions in the absence of H_2O_2 to demonstrate the reductive dissolution of each of these iron oxides at pH 4.0. Fig. 8 shows that the concentration of ferrous ions in solution increases with time for SiG1 and SiG2, but only a trace amount of ferrous ions was determined in solutions for C1 and FeOOH after 180 min. The pH does not change during the reductive dissolution of each iron oxide. This indicates that SiG1 and SiG2 are more active for reductive dissolution in the presence of catechol. The production of ferrous ions accelerates the decomposition of H_2O_2 and the degradation of phenol as the Fenton process proceeds. Based on these results, we can conclude that SiG1 and SiG2 are more actively reduced by catechol than are C1 and FeOOH. The Fe(II) is rapidly oxidized by excess H_2O_2 (Fenton's reagent) in the system, so the iron ion in the solution may be Fe(III) in complexes of organic acids. Therefore, the tendency of the dissolved iron depends on the degradation efficiency of phenol. SiG1 and SiG2 effectively catalyze the degradation of phenol by H_2O_2. Therefore, the dissolution of iron oxide and a decrease in pH were observed during the reaction (Fig. 9). However, the amount of dissolved iron was quite low and the pH was almost constant in C1 and FeOOH systems because of their inefficiency as catalysts. The degradation of phenol in SiG1 and SiG2 systems is accelerated by dissolved iron following a radical initiation of H_2O_2. Therefore, homogeneous and heterogeneous reactions proceed simultaneously. In contrast, most H_2O_2 decomposed to oxygen and water via a non-radical pathway by C1 and FeOOH. Scheme 1 exhibits the probably heterogeneous and homogeneous reactions for SiG1 and SiG2 in the presence of hydrogen peroxide and phenol. Firstly, hydrogen peroxide reacts with SiG1 or SiG2 (Fe^{III}); then, Fe^{II}, hydroperoxyl radicals and super-oxide anion radicals are produced. Phenol and some of its intermediates were degraded gradually by the Fenton process. The production of oxalic acid leads to Fe^{III} dissolution and a pH decrease. The ferrous ions and Fe^{II} are transition species and are difficult to measure in the presence of hydrogen peroxide.

4. Conclusion

Immobilized iron oxides SiG1, SiG2, and C1 on silica matrixes were withdrawn from fluidized bed reactors applied to catalyze the degradation of phenol by H_2O_2, and their effects were compared with that of the commercial catalyst FeOOH. The characterization was performed using XRD, SEM and N_2-sorption and by elucidating the kinetics of the dissolution of iron by oxalic acid in dark surroundings. XRD patterns show that SiG1, SiG2 and C1 exhibit an amorphous structure, and that FeOOH exhibits the poor crystallinity of goethite. The SEM images show that the surfaces of all of the iron oxides are smooth. The oxides are aggregated by the iron oxide floc. The N_2 adsorption isotherm reveals that SiG1 and SiG2 are non-porous materials, and that C1 and FeOOH are typical type II and typical type IV, respectively. The kinetic model of the dissolution of iron by oxalic acid is established. The apparent first-order dissolution rate constant (k_c) reveals an important property of iron oxide that is dissolved by oxalic acid. In this work, the order of apparent first-order dissolution rate constants (k_c) is SiG1 > SiG2 > FeOOH ~ C1. The immobilized iron oxides, such as SiG1 and SiG2, bond weakly with the support (silica sand) in the presence of oxalic acid. The decomposition of H_2O_2 follows pseudo-first-order kinetics. The numbers of active sites on iron oxides for the decomposition of H_2O_2 are similar among all the iron oxides at the same k_{app} (1.8×10^{-3} min^{-1}). The k_{app} provides a property of iron oxide that is related to the surface reaction with hydrogen peroxide, but it does not specify whether active radicals are generated by each one of these iron oxides. Phenol neither is adsorbed on these iron oxides nor dissolves iron from the surface of iron oxides at pH 4. SiG1 and SiG2 exhibit much greater catalytic activity in phenol degradation than either C1 or FeOOH, indicating that SiG1 and SiG2 can initiate H_2O_2 via a radical pathway and can further oxidize phenol. The reactivity of iron oxides for catalyzing

the degradation of phenol by H_2O_2 relates to the tendency of iron to be dissolved by oxalic acid. However, the apparent first-order dissolution rate constant (k_c) specifies the reactivity of iron oxide in phenol degradation. The intermediates derived from phenol degradation, such as catechol and oxalic acid, promote the dissolution of iron from SiG1 and SiG2 by reductive and non-reductive pathways, and reduce pH. The catalyses of SiG1 and SiG2 involve heterogeneous and homogeneous reactions. Furthermore, the production of active radicals, initiated by H_2O_2, involves the reductive and non-reductive dissolution of iron oxide in heterogeneous processes, while the iron ions (Fe^{2+}, Fe^{3+} and complex iron species), which react with H_2O_2 in solution, do so in homogeneous processes. In this study, we found that the main reason of iron dissolution is the formation of some organic compounds produced by phenol degradation. The mineralization of phenol and the re-immobilization of iron species will be important processes for catalyst regeneration. Recently, a photo-reactor was designed to solve the drop in pH and to control iron leaching. Those results will be published in the near future.

Acknowledgments

The authors would like to thank the National Science Council of Taiwan, for financially supporting this research under Contract No. NSC 96-2221-E-006-022 and NSC 96-2621-Z-006-017. Dr. Hung-Ta Chen is appreciated for the BET analysis. Ted Knoy is appreciated for his editorial assistance. Professor Koichi Segawa is greatly appreciated for his English corrections.

References

[1] M.I. Litter, Appl. Catal. B: Environ. 23 (1999) 89–114.
[2] N. Alhayek, M. Dore, Water Res. 24 (1990) 973–982.
[3] C.M. Miller, R.L. Valentine, Water Res. 29 (1995) 2353–2359.
[4] R.L. Valentine, H.C.A. Wang, J. Environ. Eng.-ASCE 124 (1998) 31–38.
[5] J. Guo, M. Al-Dahhan, Appl. Catal. A: Gen. 299 (2006) 175–184.
[6] W.P. Kwan, B.M. Voelker, Environ. Sci. Technol. 37 (2003) 1150–1158.
[7] K.M. Cunningham, M.C. Goldberg, E.R. Weiner, Environ. Sci. Technol. 22 (1988) 1090–1097.
[8] M.C. Lu, Chemosphere 40 (2000) 125–130.
[9] P. Baldrian, V. Merhautova, J. Gabriel, F. Nerud, P. Stopka, M. Hruby, M.J. Benes, Appl. Catal. B: Environ. 66 (2006) 258–264.
[10] F. Martinez, G. Calleja, J.A. Melero, R. Molina, Appl. Catal. B: Environ. 70 (2007) 452–460.
[11] D. Wang, Z. Liu, F. Liu, X. Ai, X. Zhang, Y. Cao, J. Yu, T. Wu, Y. Bai, T. Li, X. Tang, Appl. Catal. A: Gen. 174 (1998) 25–32.
[12] J.S. Choi, S.S. Yoon, S.H. Jang, W.S. Ahn, Catal. Today 111 (2006) 280–287.
[13] N. Crowther, F. Larachi, Appl. Catal. B: Environ. 46 (2003) 293–305.
[14] F. Martinez, J.A. Melero, J.A. Botas, M.I. Pariente, R. Molina, Ind. Eng. Chem. Res. 46 (2007) 4396–4405.
[15] J.A. Melero, G. Calleja, F. Martinez, R. Molina, M.I. Pariente, Chem. Eng. J. 131 (2007) 245–256.
[16] S. Chou, C. Huang, Y.H. Huang, Environ. Sci. Technol. 35 (2001) 1247–1251.
[17] C.L. Hsueh, Y.H. Huang, C.Y. Chen, J. Hazard. Mater. 129 (2006) 228–233.
[18] C.L. Hsueh, Y.H. Huang, C.C. Wang, C.Y. Chen, J. Mol. Catal. A: Chem. 245 (2006) 78–86.
[19] V. Kavitha, K. Palanivelu, Chemosphere 55 (2004) 1235–1243.
[20] R. Chen, J.J. Pignatello, Environ. Sci. Technol. 31 (1997) 2399–2406.
[21] G.A. Hamilton, J.W. Hanifin, J.P. Friedman, J. Am. Chem. Soc. 88 (1966) 5269–5272.
[22] Y. Du, M. Zhou, L. Lei, J. Hazard. Mater. 136 (2006) 859–865.
[23] Y.H. Huang, L.T. Cho, C.Y. Chen, Republic of China, Taiwan Patent 200616902, Ever-Clear Environmental Eng. Corp. (2004).
[24] G.M. Eisenberg, Ind. Eng. Chem. Anal. 15 (1943) 327–328.
[25] H. Tamura, K. Goto, T. Yotsuyanagi, M. Nagayama, Talanta 21 (1974) 314–318.
[26] B. Wehrli, E. Wieland, G. Furrer, Aquat. Sci. 52 (1990) 3–31.
[27] Y.W. Deng, W. Stumm, Appl. Geochem. 9 (1994) 23–36.
[28] D. Panias, M. Taxiarchou, I. Paspaliaris, A. Kontopoulos, Hydrometallurgy 42 (1996) 257–265.
[29] C.M. Miller, R.L. Valentine, Water Res. 33 (1999) 2805–2816.
[30] H. Gallard, J. De Laat, Water Res. 34 (2000) 3107–3116.
[31] J.A. Zazo, J.A. Casas, A.F. Mohedano, M.A. Gilarranz, J.J. Rodriguez, Environ. Sci. Technol. 39 (2005) 9295–9302.
[32] H.R. Devlin, I.J. Harris, Ind. Eng. Chem. Fundam. 23 (1984) 387–392.
[33] C. Liu, Y. Shan, X. Yang, X. Ye, Y. Wu, J. Catal. 168 (1997) 35–41.
[34] R. Alnaizy, A. Akgerman, Adv. Environ. Res. 4 (2000) 233–244.